

Conformational Heat Capacity of Interacting Systems of Polymer and Water

Marek Pyda

Department of Chemistry, The University of Tennessee, Knoxville, Tennessee 37996-1600, and Chemical and Analytical Sciences Division, Oak Ridge National Laboratory, Oak Ridge, Tennessee 37831-6197

Received October 23, 2001; Revised Manuscript Received March 4, 2002

ABSTRACT: Conformational contributions to the heat capacity of the interacting system of polymer–water have been studied on the example of starch with and without low concentrations of water. This work continues a series of thermal analyses of biological materials. The heat capacity has been linked to its vibrational, external, and conformational contributions. The conformational part is evaluated from a fit to a one-dimensional Ising model for two discrete states, characterized by parameters linked to stiffness, cooperativity, degeneracy, and various interactions. The changes in heat capacity within the glass-transition region are interpreted, thus, as contributions of different conformational heat capacities arising from the changes in interaction of the carbohydrate chains with water. The vibrational contribution was calculated as the heat capacity arising from group and skeletal vibrations. The external contribution was computed as a function of temperature from experimental data of the mobile state of the thermal expansivity and compressibility. The stiffness, cooperativity, and degeneracy parameters are discussed in terms of monolayers and clusters of water about the starch. The calculated and experimental heat capacities of the starch–water system are compared from 8 to 490 K, the range of measurement. The system is shown to have a glass transition of at least three steps which begin at about 250 K and are not completed at 500 K, where decomposition starts. Water plasticizes the steps of the transition differently. The proposed approach should also be usable for a more realistic description of heat capacities of other biological materials, such as the cellulose–water or protein–water systems.

Introduction

For the study the conformational heat capacity of the polymer–water system we evaluated the heat capacity in their solid, liquid, and partially mobile states within the glass transition. The conformational heat capacity is most directly coupled to the liquidlike behavior and is one of the three contributions to the total heat capacity. The other two are the vibrational contribution, which is always the largest and most important for the description of the solid state, and the so-called external contribution, which arises from the expansion of the system with temperature. For biopolymers, decomposition occurs often before the amorphous samples complete their glass transition. In these cases is not possible to measure the liquid heat capacity; rather, an estimate must be made from low-mass models, or in some cases, it may be possible to extrapolate information from the partial molar quantities of solutions in water. Water itself has a glass-transition temperature of about 140 K,¹ so that in solutions the glass-transition temperature of the polymers decreases substantially.

A number of properties of the polymer–small molecule, especially polymer–water systems, have been investigated.^{2–4} Extensive calculations for the conformations of polymer–solvent systems were carried out by Flory, Ptitsyn, Volkenstein, and co-workers.⁵ In the Flory–Huggins treatment of polymeric solutions,⁵ the volume difference between polymer and solvent and an interaction parameter χ are introduced. The interaction parameter χ is related to the heat and entropy of mixing. In cases of phase segregation, nonrandom distribution, or clustering of the small molecule, different approaches were tried by using additional functions for the description of the clustering effect.^{6–8} Tomka and co-workers^{6,7} have combined both approaches, using the Flory–

Huggins treatment for delocalized mixing and Freunlich's isotherm function to examine localized clustering in cellulose–water³ and starch–water⁷ systems. Computer simulations were also used to study the heat capacity of polymer/solvent systems.^{9,10} The magnitude of the solvation contribution to the heat capacity is well characterized experimentally in several studies.^{11–14}

To characterize the thermodynamic properties of polymer–small molecule systems, quantitative thermal analysis needs to be performed. The discussion in this paper is based on quantitative calorimetry of carbohydrates without water and with two different low concentrations of water. The data analysis is based on the advanced thermal analysis system (ATHAS).¹⁵ In addition to the description of the solid and liquid states, the quantitative thermal analysis establishes proper baselines for the discussion of phase transitions, such as the glass transition as well as ordering and disordering transitions.

The heat capacity is a macroscopic, thermodynamic quantity that is based on the molecular motion. The main contributions to the experimental heat capacity come from vibrations and large-amplitude molecular motions. The latter are mainly conformational; i.e., for flexible polymers they are caused by internal rotation. In small, rigid molecules, such as water, translational and rotational motions are the large-amplitude motions. At low temperatures, usually below the glass or melting transitions, practically only vibrations contribute to the experimental heat capacity. The vibrations in solids are separated into an approximate group vibrational spectrum, which can usually be described by a normal-mode calculation based on force constants derived from infrared and Raman spectra, and the skeletal vibrations, which can be approximated by the Tarasov equation

that is based on Debye functions of different dimensionality.¹⁵ The thus-determined vibrational heat capacity is then extended to high temperatures and serves as the baseline for quantitative thermal analysis of dry polymers and polymer–water systems. The description of the liquid heat capacities is more complicated. Empirically, it was found, however, that the heat capacity of liquid polymers is often a linear function of temperature. Furthermore, an empirical addition scheme based on contributions of the constituent chain segments could be derived within the framework of ATHAS.¹⁵ For polymer–solvent systems, an empirical addition scheme, UNIFAC, was also developed by Prausnitz and co-workers.¹⁶

There are no fully adequate and simple microscopic theories of either pure polymeric liquids or liquid polymer–small molecules system. Lattice theories are usually used for the representation of liquid structures.^{17–19} Flory,^{20–22} Sanchez,²³ and Simha^{24–26} developed the intermolecular interactions as an external contribution. Furthermore, a flexibility parameter was introduced by Prigogine²⁷ and then used by Flory,²⁰ Sanchez,^{2,23} and Simha²⁴ to describe the effect of the intramolecular interactions as a conformational contribution of the polymer. A large number of calculations of conformations of macromolecules were carried out by Flory and co-workers.²⁸ O'Reilly²⁹ considered the external and conformational contributions to the heat capacity of liquid polymers for a larger number of polymers using the rotational isomers model without a cooperative effect. Both the external and conformational contributions to heat capacity were also considered by Gibbs and DiMarzio.^{30,31} They described the vibrational contribution using an Einstein term with changes in frequencies during the glass transition. This accounted, however, only for 20% of the measured change. The approach presented here involves the calculation of the conformational contribution to the heat capacity of the amorphous polymer above glass transition and in its simplest form was first attempted for liquid polyethylene (PE)³² and then developed further for polyethylene, polypropylene, poly(methyl methacrylate), poly(*n*-butyl methacrylate), and polystyrene.³³ Good agreement between calculated and experimental data could be achieved, and a more realistic picture of the conformational behavior in linear macromolecules with longer side chains emerged. This approach is the starting point for the present analysis, and an effort will be made to estimate the liquidlike heat capacity of the polymers in the presence of low-molar-mass molecules. The starch–water system will serve as an example.

Amorphous starch was used as obtained and after various treatments, as described in the literature.^{6–8,40} Concisely, amorphous starch was prepared by extruding native potato starch obtained from Blattmann AG, Switzerland (lot 51128). In the presence of water, a process of gelatination dissolves the crystalline regions of the native starch. For potato starch this structural transformation occurs in water solution between 329 and 339 K (56 and 66 °C), in contrast to melting, where the starch crystallites would require a temperature above 443 K (170 °C). The delivered amorphous starch contained 10–12 wt % of water. It is composed of linear amylose (≈20%) and branched amylopectin (≈80%). Amylose is based on α-1,4-D-glucose units and has a molar mass from 10⁵ to 10⁶ Da. Amylopectin, in contrast, branches about once every 20–25 glucose repeat-

ing units (mainly at the C6 position, α-1,6 link) and has a typical molar mass from 10⁷ to 10⁹ Da. The repeating unit of starch (C₆H₁₀O₅) has a molar mass of 162.142 Da.

To obtain dry starch, the sample was held in a vacuum oven at 353 K (80 °C) for a minimum of 48 h. To introduce fixed amounts of water, either small amounts were added to the dry starch or the dry starch was kept for 2–3 weeks in contact with the constant saturated vapor pressure of the following salt solutions of appropriate concentration: lithium chloride (10% RH), magnesium chloride (33% RH), sodium bromide (57% RH), sodium chloride (75% RH), and potassium chloride (86% RH). The uptake of water by the starch was measured by weighing the sample with a microbalance (Cahn C-33). The dry sample had the same mass before and after the DSC measurements with a margin of error of ±0.005 mg. The heat capacity of starch–water with samples containing 53 mol % (11 wt %) and 65 mol % (17 wt %) of water was measured and analyzed for this paper. The samples were sealed in high-pressure stainless steel pans (HPS) from the Perkin-Elmer Corp., Norwalk, CT, to prevent water loss during measurements by standard DSC.

Calculation Scheme

Conformational Contribution to the Heat Capacity of Dry Polymer. Generally, the heat capacity of the liquid polymer is calculated from the standard thermodynamic relationship:^{33,36}

$$C_p = C_v + TV\alpha^2/\beta_c \approx C_{\text{vib}}(\text{poly}) + C_{\text{conf}}(\text{poly}) + C_{\text{ext}}(\text{poly}) \quad (1)$$

where C_p represents the liquid heat capacity at a constant pressure, C_v the heat capacity at constant volume, V the molar volume, α the thermal expansivity, and β_c the compressibility. All quantities must be known or estimated as a function of temperature. The experimental heat capacity C_p of dry polymer is, thus, separated into a vibrational heat capacity $C_{\text{vib}}(\text{poly})$, the conformational heat capacity $C_{\text{conf}}(\text{poly})$, and the so-called external contribution $C_{\text{ext}}(\text{poly})$. For the heat capacities of polymeric solids below about 150 K, eq 1 is reduced to $C_{\text{vib}}(\text{poly})$ since the chain conformation is largely rigid, and $C_{\text{ext}}(\text{poly})$ is small. At somewhat higher temperature, the small $C_{\text{ext}}(\text{poly})$ for the solid state can often be estimated using the Nernst–Lindemann equation or similar approximations if expansivity and compressibility are not known.^{37,38} Both of these contributions yield the baseline above which $C_{\text{conf}}(\text{poly})$ is found. Above about 50 K, crystalline and amorphous polymers, as well as polymers of intermediate crystallinity, have similar heat capacities. They can be calculated as³³

$$C_{\text{vib}}(\text{poly}) = C_v(\text{group}) + C_v(\text{sk})[\Theta_1, \Theta_2, \Theta_3] \quad (2)$$

where $C_v(\text{group})$ is the heat capacity based on the group-vibrational spectrum and $C_v(\text{sk})$ is the heat capacity for the skeletal vibrations, estimated using the ATHAS scheme.^{15,34,35} The parameters Θ_1 , Θ_2 , and Θ_3 represent the characteristic one-, two-, and three-dimensional Debye frequencies for continua, which are expressed in kelvin ($\Theta = h\nu/k_B$). The internal rotation which is involved in the conformational motion changes its heat capacity only very slowly from the limit of torsional

oscillation ($8.314 \text{ J K}^{-1} \text{ mol}^{-1} = R$) to a free rotator ($C_v = R/2$) but may involve larger changes in potential energy, which will be discussed next using a simple energy-level scheme.

Calculation of the conformational contribution to the liquid heat capacity of polymers $C_{\text{conf}}(\text{poly})$ in eq 1 is based on the earlier calculation³³ of the conformational contribution of the dry polymer, using one-dimensional Ising model³⁹ with the following simplifying assumption: The conformational states of the bonds can occur in only two discrete states, a ground state and an excited state, with the energy difference between the two states B , which can be modified with a parameter A , depending on the state of the next-nearest neighbors; depending on the cooperative interactions, it may be positive or negative. Thus, the parameters B and A account for stiffness and cooperativity. The conformations of the whole chain of a polymer with a total of N rotatable bonds are then described by the one-dimensional Ising model^{33,39} with the total potential energy:

$$E_1 = A \sum_{j=1}^N m_j m_{j+1} + B \sum_{j=1}^N m_j \quad (3)$$

The conformation number $m_j = 0$ applies to the ground state with energy zero and degeneracy g_0 . The conformation number $m_j = 1$ corresponds to the excited state with energy B and degeneracy g_1 . The ratio of the degeneracy of the conformational states $g_1/g_0 = \Gamma$, and the energies A and B are determined by the fit to the experimental conformational heat capacity calculated from eq 1.

Knowing E_1 , as given by eq 3, one can calculate the partition function and the free energy per bond using the transfer-matrix method,³⁹ and finally, the conformational heat capacity can be expressed in closed form as³³

$$C_{\text{conf}}(\text{poly}) = R \frac{(g_1/g_0)[B/(k_B T)]^2 e^{-B/(k_B T)}}{[(g_1/g_0)e^{-B/(k_B T)} + 1]^2} [1 + \vartheta(A, B, \Gamma, T)] \quad (4)$$

where the first part of the equation is identical to the rotational isomers model;^{29,33,36} the second expression $\vartheta(A, B, \Gamma, T)$ is too extensive to be shown in detail but gives contributions from the interaction of the nearest conformational neighbors. In eq 4, R is the gas constant, k_B is the Boltzmann constant, and T is the temperature in kelvin. A full description of this calculation was given earlier³³ and will be used to calculate the conformational contribution to the heat capacity of pure, amorphous, dry starch. The total heat capacity of the pure liquid polymers is then estimated from eq 1, using the experimental data for $C_{\text{ext}}(\text{poly})$.

Conformational Contribution to the Heat Capacity of the Polymer–Small Molecules Systems. The calculation of the heat capacity of the liquid solution of amorphous polymers and small molecules is based on the evaluation of

$$C_p(\text{poly-sm}) = C_{\text{vib}}(\text{poly-sm}) + C_{\text{conf}}(\text{poly-sm}) + C_{\text{ext}}(\text{poly-sm}) \quad (5)$$

where $C_p(\text{poly-sm})$ represents the total heat capacity at constant pressure for the system polymer/small molecules, $C_{\text{vib}}(\text{poly-sm})$ is the vibrational heat capacity

at constant volume, $C_{\text{ext}}(\text{poly-sm})$ stands for the external heat capacity, and $C_{\text{conf}}(\text{poly-sm})$ denotes the conformational heat capacity.

The major part of the total heat capacity, again, comes from the vibrational motion as given earlier.⁴⁰ The value of $C_{\text{vib}}(\text{poly-sm})$ can be estimated by adding the contributions for the polymer $C_{\text{vib}}(\text{poly})$ and the small molecules, $C_{\text{vib}}(\text{sm})$, according to the equation

$$C_{\text{vib}}(\text{poly-sm}) = X_S C_{\text{vib}}(\text{poly}) + X_W C_{\text{vib}}(\text{sm}) \quad (6)$$

where X_S and X_W are the molar fractions of polymer repeating units and small molecules, respectively.⁴⁰ The external contribution to the heat capacity, $C_{\text{ext}}(\text{poly-sm})$ of eq 5, is calculated using the experimental molar volume V , the thermal expansivity α , and the compressibility β_c , as before. The calculation of the conformational contribution to the liquid heat capacity of the polymer–small molecules complex is based on the description for pure polymers³³ and is presented next.

Calculation of the Conformational Heat Capacity of the Polymer–Small Molecules System. As a starting point for the calculation of the conformational heat capacity of the polymer–small molecule system, let us first consider monolayers of small molecules surrounding the polymer chain. This will be followed by a model involving clusters of small molecules which interact with the flexible macromolecule. The assumptions are again that the conformational states of the polymer are discrete and can be represented by only two states as in a simplified rotational isomers model.^{29,33,36} Each of the conformational states can be degenerate in multiple ways, and we neglect any excluded-volume effects.⁵ To describe the conformational energy of the chain, the one-dimensional Ising model is used again,³⁹ but with the following change: The conformational states of each chain segment depends besides on the adjacent segments also on the interaction with the small molecules in the immediate neighborhood. Consequently, if the conformations of different polymer segments are mutually dependent, the small molecules can interact indirectly with other small molecules through the conformations of the chain segments. This interaction leads to cooperative effects which should be reflected in the heat capacity of the system.

According to the above assumption there are, again, N identical segments of the polymer, and there are also N centers for the small molecules. Each segment can be found in one of two conformational states, and each state can be degenerate. The ground state has the degeneracy g_0 and is characterized by a zero energy, while the excited state has the degeneracy g_1 and has the energy $B > 0$. The ratio is $\Gamma = g_1/g_0$ as before. The value of B is modified by A but depends not only on the states of neighboring segments but also on the cooperative behavior of the monolayer of the small molecules on the polymer, having the energy $E < 0$. In the case of clusters of small molecules, the second and higher layers have the same energy K_1 , where $K_1 \leq 0$ and s is the maximum number of molecules in the cluster. Each interaction energy of the small molecules with the segment of the polymer, E , can be modified by a parameter C , if the next segment of the chain is in the excited state. The energy C describes then the coupling between the conformational states and the small molecules. If the segment of the chain and its neighboring small molecule are considered as one center, the energy of the whole system can be represented as follows:

(a) for monolayers ($s = 1$):

$$E_{I_1}(\text{poly-sm}) = A \sum_{j=1}^N m_j m_{j+1} + B \sum_{j=1}^N m_j + C \sum_{j=1}^N m_j n_j + (E - \mu) \sum_{j=1}^N n_j \quad (7)$$

(b) for cluster ($s > 1$):

$$E_{I_s}(\text{poly-sm}) = A \sum_{j=1}^N m_j m_{j+1} + B \sum_{j=1}^N m_j + C \sum_{j=1}^N m_j (1 - \delta_{n_j 0}) + (E - K_1) \sum_{j=1}^N \sum_{n'=1}^s \delta_{n_j n'} + (K_1 - \mu) \sum_{j=1}^N \sum_{n'=1}^s n_j \delta_{n_j n'} \quad (8)$$

In eqs 7 and 8, $K_1 = K - \Delta K$ is the energy at the intermediate state related to the condensation energy K of a small molecule, and μ is the chemical potential of small molecules. Each site of the model is described by the pair of numbers (m_j, n_j) , where conformational number $m_j = 0$ corresponds to the ground state with degeneracy g_0 , and $m_j = 1$ corresponds to an excited state with degeneracy g_1 for the j th segment. In eq 7, the occupation number for small molecules n_j can only take the value 0 for an empty center and 1 for an occupied center ($s = 1$ for monolayers). For cluster of small molecules in eq 8, the occupation number $n_j = 0, 1, 2, 3, \dots, s$ refers to an empty center (0) or the center occupied by 1, 2, 3, ..., and s small molecules with energies states 0, E , $E + K_1$, ..., $E + (s - 1)K_1$, respectively. Each site of the system can be in $(g_1 + g_0) - (s + 1)$ states. In eq 8, δ is the Kronecker delta. Several sites of the possible conformational states of the polymer–small molecules system are presented schematically in Figure 1.

The conformational free energy F_{conf} per site for the systems is calculated using the transfer matrix method:³⁹

$$F_{\text{conf}} = -k_B T \ln \Xi = -k_B T \ln [\text{Tr } e^{-(E_I(\text{poly-sm})/k_B T)}] \quad (9)$$

where Ξ is the partition function and $E_I(\text{poly-sm})$ is given by eqs 7 or 8. The result has the form

$$F_{\text{conf}} = -(\beta N)^{-1} \ln P_{\text{max}}^N = -(\beta)^{-1} \ln \frac{1}{2} [U + (U^2 - 4V)^{0.5}] \quad (10)$$

where

$$U = 1 + ab' + k_1 k_2 x (1 + ab'c) \left[\frac{1 - (k_2 x)^2}{1 - k_2 x} \right] \quad (11a)$$

$$V = (ab' - b) \left[1 + k_1 k_2 x (1 + ab'c) \frac{1 - (k_2 x)^2}{1 - k_2 x} \right] \left[1 + ck_1 k_2 x (1 + ab'c) \frac{1 - (k_2 x)^2}{1 - k_2 x} \right] \quad (11b)$$

The parameters k_1 , k_2 , a , b' , and c are defined by the following relationships:

$$a = \exp(-\beta A); b' = \Gamma b = \Gamma \exp(-\beta B); c = \exp(-\beta C) \\ k_1 = \exp[-\beta(E - K_1)]; k_2 = \exp[-\beta(K - K_1)]$$

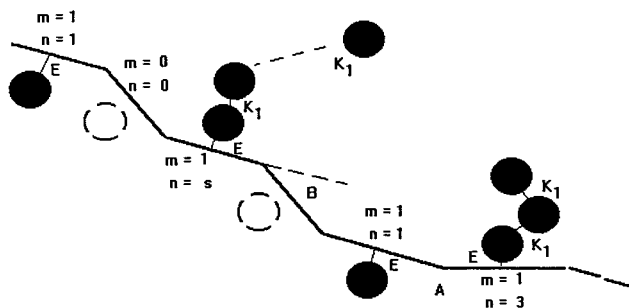


Figure 1. Schematic diagram of conformational states of several sites in the polymer surrounded by small molecules.

with $\beta = (k_B T)^{-1}$ and $\Gamma = g_1/g_0$; $\text{Tr } \exp[-\beta E_I(\text{poly-sm})]$ in eq 9 denotes the trace of the matrix. The quantity $x = \exp[-\beta(K - \mu)]$ has the meaning of an activity of small molecules.

Knowing F_{conf} from eq 10, it is possible to calculate all thermodynamic quantities of the system. The conformational heat capacity $C_{\text{conf}}(\text{poly-sm})$ is given by

$$C_{\text{conf}}(\text{poly-sm}) = \frac{dU_{\text{conf}}}{dT} \\ U_{\text{conf}} = -k_B T^2 \frac{d(F_{\text{conf}}/k_B T)}{dT} = -k_B T^2 \frac{d(\ln \Xi)}{dT} \quad (12)$$

where U_{conf} is the conformational enthalpy of the system.

The calculation of the heat capacity is rather tedious because of the double differentiation of the partition function. This calculation was done using the Mathematica 3.0 software. The final results can be expressed in a closed form as the conformational heat capacity, but the expression is too long to be shown here.

The conformational heat capacity in eq 12 is a function of temperature with many parameters, i.e., $C_{\text{conf}}(\text{poly-sm}) = f(T, B, A, C, E, \Gamma, K_1, K, s)$ where B, A, Γ, C describe the polymer and E, K_1, K, s the small molecules. These parameters can be estimated from experimental data or from additional models generated.

The heat capacity in the liquidlike state of the polymer–small molecule system is then estimated similar as for the pure polymer, by finding the sum of the vibrational, external, and conformational contributions. The experimental conformational heat capacity is fitted to the calculated $C_{\text{conf}}(\text{poly-sm})$ obtained from eq 12 of the Ising model to obtain the parameters $B, A, C, E, \Gamma, K_1, K$, and s for the system of polymer and small molecules.

Results and Discussion

The quantitative thermal description of the starch–water system starts with the analysis of the experimental heat capacities. Figure 2 shows these as specific heat capacities, measured by adiabatic calorimetry and differential scanning calorimetry from 8 to 490 K.⁴⁰ The detailed data are also available through the ATHAS Data Bank.¹⁵ A comparison with the expected values for the liquid samples has clearly shown that the glass transitions between about 200 and 372 K are only partial and occur in stages and that even the dry starch shows the first of these stages.⁴⁰ The heat capacities below the glass transition were linked to the vibrational motion.⁴⁰ The additional large-amplitude motions and

Table 1. Fitting Parameters for the Conformational Heat Capacities of Starch and Starch–Water Systems^a

water content (mol %)	<i>B</i> (K)	<i>A</i> (K)	Γ	<i>s</i>	<i>C</i> (K)	<i>K</i> − μ (K)	<i>E</i> − <i>K</i> ₁ (K)	<i>K</i> − <i>K</i> ₁ (K)	temp (K)
dry starch	2400	364	113						380–436
starch–water									
53 ^b	2400	364	148	0.74	−369	−1343	690	1156	305–355
53 ^c	2400	364	1890	0.74	−1680	−1398	1378	1367	390–436
65	2400	364	224	2.8	−1567	−1347	1234	1177	330–380

^a The values of *B*, *A*, *C*, *K* − μ , *E* − *K*₁, and *K* − *K*₁ are in terms of temperatures, given in kelvin. ^b Describes the range of lower temperature in the fitting as shown in Figure 4. ^c Describes the range of higher temperature in the fitting as shown in Figure 4.

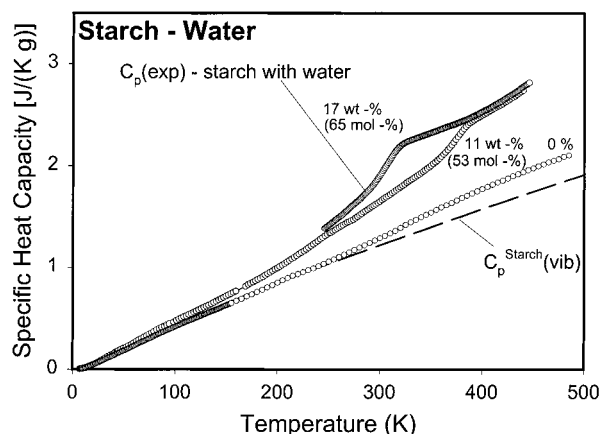


Figure 2. Experimental specific heat capacities of the starch–water system. The water concentrations are listed in the figure; *C_pstarch(vib)* is the vibrational, calculated, specific heat capacity of dry starch.⁴⁰

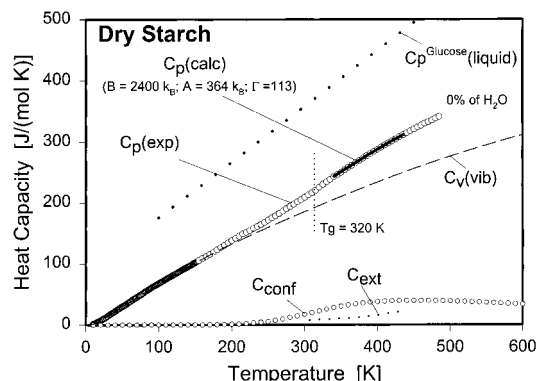


Figure 3. Comparison of the experimental and calculated heat capacities for dry starch.

increased external contribution after each of the partial glass transitions are the subject of the present discussion.

Heat Capacity of Amorphous Dry Starch. The heat capacity of the amorphous, dry starch above the partial glass transition can be analyzed with eqs 1–4, as is shown in Figure 3. The fitting parameters are listed in Table 1. Figure 3 shows a good agreement of experimental and calculated *C_p*. The experimental data in the temperature range from 320 to 436 K were separated as indicated by eq 1. The vibrational heat capacity was calculated as before.^{33,40} For the external heat capacity contribution, *C_{ext}*(poly), eq 3 was used with the expansivity ($\alpha = -d \ln V/dT$) and the compressibility ($\beta_c = d \ln V/dP$), derived from the experimental *P*–*V*–*T* diagram.^{6–8} The conformational contribution to total heat capacity of dry starch was then fitted to eq 4 after subtracting the vibrational and external portions of heat capacity to find the three characteristic parameters, *B*, *A*, and Γ which are listed in Figure 3 and Table 1.

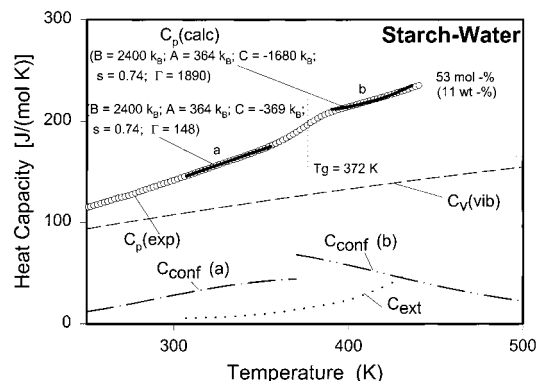


Figure 4. Comparison of the experimental and calculated heat capacities for starch with 53 mol % of water.

Adding calculated *C_{conf}*(poly), vibrational, and external heat capacities, the total, calculated heat capacity was computed, as is illustrated in Figure 3. Note that the parameters *A* and *B* are given in terms of Θ temperatures in kelvin, so that the energy *B* of 2400 K is obtained in units of J mol^{−1} by multiplication with the gas constant *R* = 8.314 J K^{−1} mol^{−1} (= 20 kJ mol^{−1}). The effective energy between the two conformational states *B* + *A* = 23 kJ mol^{−1} is rather high, which suggests that the segments or bonds in the glucose unit are rather stiff, as expected from the abundant hydrogen bonds. The value of the degeneracy ratio $\Gamma = 113$ for dry starch refers to the number of conformational isomers of four bonds (3⁴) from the total of 12 potentially mobile bonds in a residue of glucose. This is a similar value as derived from the experimental change of the heat capacity at *T_g* (32.7 kJ mol^{−1} K^{−1}). This value corresponds to three mobile bonds in the glucose repeating unit when applying the empirical rule that each bond that becomes mobile at the glass transition contributes about 11 J K^{−1} mol^{−1} to ΔC_p .^{33,40}

Heat Capacity of Amorphous Starch–Water Systems. Figures 4 and 5 show the comparison of the experimental and calculated heat capacities of starch with water in the glass transition region. For both cases the experimental data of heat capacity at constant pressure have been separated according to eq 5. The vibrational heat capacity at constant volume *C_{vib}*(poly-sm) [dashed lines in Figures 4 and 5] was estimated by adding the vibrational heat capacity from dry starch, *C_vstarch(vib)*, and the vibrational contribution from glassy water, *C_pglassy water(vib)*, as given in detail earlier:⁴⁰

$$C_v(\text{vib}) = X_S C_v^{\text{starch}}(\text{vib}) + X_W C_v^{\text{glassy water}}(\text{vib}) \quad (13)$$

where *X_S* and *X_W* are the molar fractions of starch and water, respectively.

For the calculation of the external heat capacity, *C_{ext}*(poly-sm), the second part of the center of eq 1 was used, with *V* the total molar volume, α the thermal

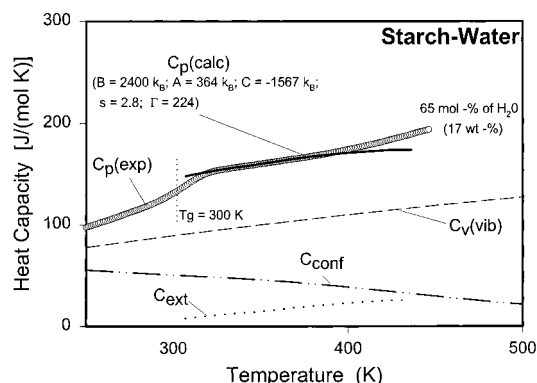


Figure 5. Comparison of the experimental and calculated heat capacities for starch with 65 mol % of water.

expansivity, and β_c the compressibility for starch with 53 and 65 mol % of water, respectively, as is available in the literature.^{6–8} Figure 6a–c shows plots for the data used. The results of the external heat capacity are drawn in Figures 4 and 5 as dotted lines.

The conformational heat capacity of starch–water systems, $C_{\text{conf}}(\text{poly-sm}) = f(T, B, A, C, E, \Gamma, K_1, K, s)$, was fitted to the experimental conformational contribution setting B and A to the values obtained for the dry starch. From the experimental heat capacities of starch–water the vibrational and external portions of the heat capacity were subtracted, and the remaining conformational part was fitted as outlined above. The parameters obtained from the fitting are listed in Table 1 and also shown in part in Figures 4 and 5. Finally, the vibrational, conformational, and external heat capacities were added, and the total heat capacity was calculated and shown in Figures 4 and 5 as the heavy lines. The root-mean-square deviations of the experimental heat capacity from the calculated values are always less than $\pm 2\%$ and depend on the temperature ranges used.

In Figure 4, from the best fit from 390 to 445 K (region *b*), the effective energy difference between the two conformational states $B + A + C = 1084$ K (9.01 kJ mol^{−1}) is reduced from the 23 kJ mol^{−1} for dry starch—a result one would expect since the presence of water should increase the flexibility. Also, the best fit in region (*b*) gives a total number of 0.74 molecules of water per glucose repeating unit (s), a value not far from 1.13 expected for the experimental 53 mol % of water since no crystallizable water was detected.⁸ The value of the degeneracy ratio Γ is 1890 and corresponds to a number of conformational isomers of almost seven bonds (3^7) compared to the four in dry starch. The added mobility must be caused by the water. It corresponds also to the larger experimental change of the heat capacity in this section of the glass transition [$\Delta C_p^{\text{AB}} = 67.4$ J K^{−1} mol^{−1}, see Figure 6 in ref 40]. The values of other parameters such as energies of E and K_1 correspond to water–carbohydrate and water–water interactions, respectively.

In addition, the experimental heat capacity of starch with 53 mol % water was fitted below $T_g = 372$ K, from 305 to 355 K (region *a* in Figure 4), using the fixed values of B , A , and s from above. The best fit gives an effective energy of 20 kJ mol^{−1} ($B + A + C = 2395$ K), which is higher than the value in region *b* due to the lower absolute value of the coupling parameter C ($= -369$ K). The effective stiffness of the carbohydrate chain becomes higher than in region *b* due to some frozen motion of the starch–water system. The value of $\Gamma = 148$ gives the suggestion that only 3 – 4 bonds per residue of glucose of starch are mobile. The difference of conformational contributions between $C_{\text{conf}}(\text{b})$ and $C_{\text{conf}}(\text{a})$ at the lower partial glass transition is, again, similar to the jump in heat capacity ΔC_p in the experimental data. The changes of the effective stiffness of chain carbohydrate below and above the glass transition can also be related to a change of the population of

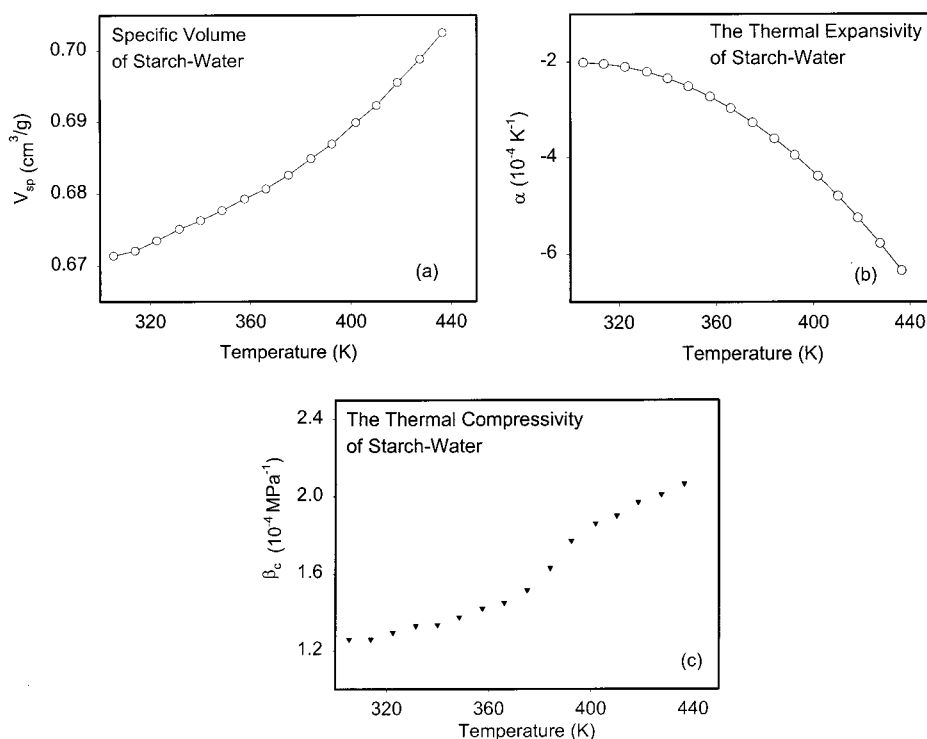


Figure 6. Experimental specific volume (a), expansivity (b), and compressibility (c) as a function of temperature for starch with 53 mol % of water.^{6–8}

secondary bonds between the carbohydrate chain. The coupling parameter C can indirectly describe this process through the secondary subsystem which was fixed in our model. Figure 4 in the temperature range 305–445 K demonstrates a good agreement between both experimental and calculated heat capacity at constant pressure when assuming two steps of a glass transition which, however, is still incomplete at 445 K.

In Figure 5 the data for 65 mol % of water are analyzed. For this sample the water has moved the second glass transition step more than the first, so that now both seem to occur at about 300 K. In addition above about 400 K a further increase in glass transition seems to signal the last step of the glass transition, lowered by the water sufficiently to fall below the decomposition temperature. Again, a good agreement exists between calculated and experimental data between 330 and 380 K. For the calculation of the heat capacity for the partially liquidlike state was estimated in the same manner as before. The vibrational contribution according to eq 13 is given by the dashed line in Figure 5, and the external contribution is plotted as the dotted line. All parameters are listed in Table 1. As in Figure 4, B and A parameters were fixed to the dry starch values. The effective energy difference between the two conformational states is 10 kJ mol^{-1} ($B + A + C = 1197 \text{ K}$), similar as in region b of Figure 4. This means that adding water beyond 53 mol % does not increase the flexibility of the carbohydrate chain. From the best fit, the value of Γ was reduced to 224 compared to 1890 for starch with 53 mol % of water so that it corresponds to a number of conformational-isomers of almost five bonds (3^5). This should be related to the increasing of numbers of water molecules per glucose unit in the starch–water system. From the best fit, $s = 2.8$, the maximum number of water molecules that can interact with one glucose unit is very close to the expected value: 3.0. This comparison to the experimental value of 1.9 molecules per glucose residue for 65 mol % of water in starch shows that still is enough space to saturate the system.

Conclusions

Attempting for the first time a quantitative thermal analysis of starch and starch water has led to the surprising discovery that the glass transition of dry starch is rather broad and does not occur in its entirety above the decomposition; rather, it starts gradually at about 200 K as illustrated in Figure 3. The heat capacity reaches only an estimated 30% of the total ΔC_p at 400 K. On adding water to the amorphous starch this first step of the glass transition moves to lower temperature and develops at 53 mol % a second, somewhat more prominent step at 372 K, shown in Figure 4. Increasing the water content to 65 mol % (Figure 5) shows that this step moves to about 300 K, allowing little of the intermediate region possible to discern as region a in Figure 4. Finally, in Figure 5 there is some indication that the third step begins at this water concentration at about 400 K.

The vibrational contribution could be assessed from the low-temperature heat capacity, the external part measured, and the conformational part was shown to be representable with a one-dimensional Ising model. The water was to a large degree accounted for as being attached to the starch chain, increasing initially its flexibility. No water is sufficiently free to crystallize. The

lowering of the glass transition is larger for the higher-temperature stages of the transition, as expected from the low level of the water glass transition. Our approach not only leads to a good fit of the data but also gives a more realistic picture of the conformational behavior in the starch–water systems and can probably also be applied to other synthetic and biological polymer–small molecule systems.

Acknowledgment. The author thanks Prof. Bernhard Wunderlich for suggestions, comments, and discussions. This work was supported by the Division of Materials Research, National Science Foundation, Polymers Program, Grant DMR-9703692, and the Division of Materials Sciences, Office of Basic Energy Sciences, U.S. Department of Energy at Oak Ridge National Laboratory, managed and operated by UT-Battelle, LLC, for the U.S. Department of Energy, under Contract DOE-AC05-00OR22725.

References and Notes

- (1) Sugisaki, M.; Suga, H.; Seki, G. *Bull. Chem. Soc. Jpn.* **1968**, *41*, 2591.
- (2) Sanchez, I. C. *Physics of Polymers Surfaces and Interfaces*; Butterworth-Heinemann: Stoneham, MA, 1992. De Gennes, P. G. *Scaling Concepts in Polymers Physics*; Cornell University Press: Ithaca, NY, 1979. Khongtong, S.; Ferguson, G. S. *J. Am. Chem. Soc.* **2001**, *123*, 3588.
- (3) Beck, M. I.; Tomka, I. *J. Macromol. Sci., Phys.* **1997**, *B36* (1), 19. Trommsdorff, U.; Tomka, I. *Macromolecules* **1995**, *28*, 6138.
- (4) Privalov, P. L. *Adv. Protein Chem.* **1995**, *33*, 167. Pfeil, W. *Thermodynamic Data of Biochemistry and Biotechnology*; Springer-Verlag: Berlin, 1986; pp 349–376. Sturtevant, J. M. *Annu. Rev. Phys. Chem.* **1987**, *38*, 463. Maeda, Y.; Nakamura, T.; Ikeda, I. *Macromolecules* **2001**, *34*, 1391.
- (5) Flory, P. J. *Principles of Polymers Chemistry*; Cornell University Press: Ithaca, NY, 1953. Birshtein, T. M.; Pitsyn, O. B. *Conformations of Macromolecules*; Interscience: New York, 1966. Volkenstein, M. V. *Configurational Statistics of Polymer Chains*; Interscience: New York, 1963.
- (6) Benczedi, D.; Tomka, I.; Escher, F. *Macromolecules* **1998**, *31*, 3055.
- (7) Benczedi, D.; Tomka, I.; Escher, F. *Macromolecules* **1998**, *31*, 3062.
- (8) Benczedi, D. Thesis, ETH Zurich, Switzerland, 1995.
- (9) Madan, B.; Sharp, K. *J. Phys. Chem.* **1996**, *100*, 7713.
- (10) Spolar, R. S.; Record, M. T. *Science* **1994**, *263*, 777.
- (11) Makhatadze, G.; Privalov, P. *J. Mol. Biol.* **1990**, *213*, 385.
- (12) Hatakeyama, H.; Hatakeyama, T. *Thermochim. Acta* **1998**, *308*, 3.
- (13) Takahashi, H.; Aoki, H.; Inoue, H.; Kadama, M.; Hatta, I. *Thermochim. Acta* **1998**, *308*, 85; **1997**, *303*, 93.
- (14) Mrevlishvili, G. M.; Metreveli, N. O.; Razmadze, G. Z.; Mdzinashvili, T. D.; Kakabadze, G. R.; Khvedelidze, M. M. *Thermochim. Acta* **1998**, *308*, 41.
- (15) General description: Wunderlich, B. *Pure Appl. Chem.* **1995**, *67*, 1919. For detailed information of the computed heat capacities, see our World Wide Web address on the Internet, the ATHAS data bank, M. Pyda, Ed.: web.utk.edu/~athas. For experimental heat capacities, see: Gaur, U.; Lau, S.-F.; Shu, H.-C.; Wunderlich, B. B.; Varma-Nair, M.; Wunderlich, B. *J. Phys. Chem. Ref. Data* **1981**, *10*, 89, 119, 1001, 1051; **1982**, *11*, 313, 1065; **1983**, *12*, 29, 65, 91; **1991**, *20*, 349.
- (16) Oishi, T.; Prausnitz, J. M. *Ind. Eng. Chem. Process Des. Dev.* **1978**, *17*, 333.
- (17) Eyring, H. *J. Chem. Phys.* **1936**, *4*, 283.
- (18) Cernuschi, F.; Eyring, H. *J. Chem. Phys.* **1939**, *7*, 547.
- (19) Lennard-Jones, J. E.; Devonshire, A. F. *Proc. R. Soc. London* **1937**, *A163*, 53; **1938**, *A165*, 1.
- (20) Flory, P. J. *J. Am. Chem. Soc.* **1964**, *86*, 1833.
- (21) Flory, P. J.; Orwal, R. A.; Vrij, A. *J. Am. Chem. Soc.* **1964**, *86*, 3507.
- (22) Eichinger, B. E.; Flory, P. J. *J. Trans. Faraday Soc.* **1968**, *64*, 2305.
- (23) Sanchez, I. C.; Lacombe, R. H. *J. Phys. Chem.* **1976**, *80*, 2352. Sanchez, I. C.; Cho, J. *Polymer* **1995**, *36*, 2929. Cho, J.; Sanchez, I. C. *Macromolecules* **1998**, *31*, 6650.

- (24) Simha, R.; Somcynsky, T. *Macromolecules* **1969**, *2*, 342.
(25) Simha, R. *Macromolecules* **1977**, *10*, 1025.
(26) Simha, R. *Ann. N.Y. Acad. Sci.* **1976**, *2*, 279.
(27) Prigogine, I.; Trappeniers, N.; Mathot, V. *Discuss. Faraday Soc.* **1953**, *15*, 93.
(28) Selected works of: Flory, P. J. *Chain Configuration and Dependent Properties*; Academic Press: Stanford, 1985; Vol. II, Part 4.
(29) O'Reilly, J. M. *J. Appl. Phys.* **1977**, *48*, 4043.
(30) Gibbs, J. H.; DiMarzio, E. A. *J. Chem. Phys.* **1956**, *25*, 185.
(31) Gibbs, J. H.; DiMarzio, E. A. *J. Chem. Phys.* **1958**, *28*, 373, 807; *J. Polym. Sci.* **1959**, *40*, 121; *J. Appl. Phys.* **1979**, *50*, 6061.
(32) Loufakis, K.; Wunderlich, B. *J. Phys. Chem.* **1988**, *92*, 4205.
(33) Pyda, M.; Wunderlich, B. *Macromolecules* **1999**, *32*, 2044.
(34) Wunderlich, B. *J. Phys. Chem.* **1962**, *37*, 1207.
(35) Pyda, M.; Bartkowiak, M.; Wunderlich, B. *J. Therm. Anal.* **1998**, *52*, 631.
(36) Wunderlich, B. *Thermal Analysis*; Academic Press: Boston, 1990.
(37) Nernst, W.; Lindemann, F. A. *Z. Electrochem.* **1911**, *17*, 817.
(38) Pan, R.; Varma-Nair, M.; Wunderlich, B. *J. Therm. Anal.* **1989**, *35*, 955.
(39) Huang, K. *Statistical Mechanics*; Wiley: New York, 1963.
(40) Pyda, M. *J. Polym. Sci., Part B: Polym. Phys.* **2001**, *39*, 3038.

MA0118466